

A New Stiffness Evaluation toward High Speed Cell Sorter

Yuki Hirose, Kenjiro Tadakuma, Mitsuru Higashimori, Tatsuo Arai, Makoto Kaneko
Ryo Iitsuka, Yoko Yamanishi, and Fumihito Arai

Abstract—Cell stiffness could be an index for evaluating its activity. Although various systems measuring cell stiffness have been proposed so far, they are slow for adaptively connecting to cell sorters capable of handling more than 1000 [cells/sec]. This paper proposes a new approach that can indirectly evaluate the cell stiffness by measuring the passing time for a narrow channel. When a cell passes through the channel, it receives a viscous force depending upon how much deformation is exerted on the cell. We show that the stiffness is a function of both the passing time and the initial diameter of cell. We also show that the stiffness is proportional to the passing time and inversely proportional to the initial diameter, under the assumption that the thickness of fluid film is inversely proportional to the normal force. The experimental validation is given together with the basic working principle.

I. INTRODUCTION

Tissue engineering enables us to recover our damaged tissues that can not be recovered naturally by their own life power. For such tissue engineering, a big expectation is given to both ES and iPS cells, since they could be any possible organ, such as cornea, heart, lung, skin, bone and so forth after numerous number of cell separation [1]. ES cells are created from the blastocyst in early embryos [2], and iPS cells are produced by introducing specific genes into biological cells [3]. These artificial cells have both self-renewal and multilineage potentials, which are essential for restoration of tissue. However, all cells do not always grow up successfully. Only a limited percentage of cells can survive and eventually form a shape for transferring to human body. So far, the selection of cells toward a further process is mostly done by technicians with their experiences and six senses. In order to keep quality of tissues before transferring to a further treatment, a quantitative index has been strongly required. While it is normally hard for us to evaluate the activity level of each cell, we can naturally expect that there exists a correlation between the activity level and the cell stiffness. This is the starting point in this work. As for sensing of cell stiffness, there are various approaches. The most popular one is perhaps the utilization of AFM (Atomic Force Microscope) [4]–[7] where we can

This work is partially supported by g-COE in-Silico Medicine(Osaka University)

Y. Hirose, K. Tadakuma, M. Higashimori, T. Arai and M. Kaneko are with the Department of Mechanical Engineering, Osaka University, 2-1 Yamadaoka, Suita, Osaka, 565-0871, JAPAN. {hirose, tadakuma, higashi, mk}@hh.mech.eng.osaka-u.ac.jp, arai@sys.es.osaka-u.ac.jp

R. Iitsuka, Y. Yamanishi and F. Arai are with the Department of Bioengineering and Robotics, Tohoku University, Aramaki Aza Aoba 6-6-01, Aoba-ku, Sendai, Miyagi, 980-8579, Japan. {iitsuka, yamanishi, arai}@imech.mech.tohoku.ac.jp

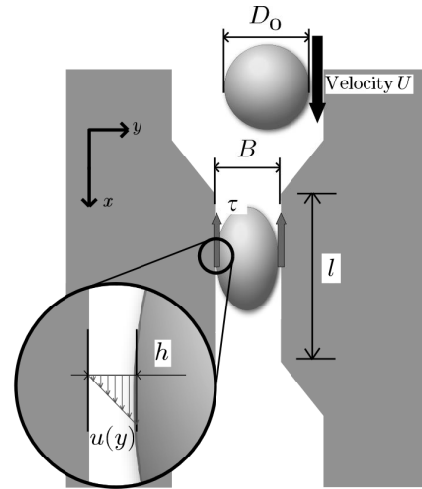


Fig. 1. Cell and microchannel model

compute the Young's modulus by the relationship between the bending motion of cantilever after making contact with cell and the displacement of the tip of cantilever. However, for completing the whole procedure, this approach takes time in the order of several minutes at least. S. Omata et. al. have proposed the measure system for bovine ovum by using Micro Tactile Sensor (MTS) [8], which inserts a probe into a cell to the extent about 5 [μm] to obtain the tactile information such as local elasticity. T. Matsumoto et. al. have discussed a pulling based stiffness measurement where a smooth muscle cell is pulled by two micro glass pipettes, and the stiffness is evaluated by measuring the pulling force as well as the total displacement [9].

We are planning to connect the stiffness sensing system with the cell sorter with the speed in the order of less than msec. From the viewpoint of high speed sensing, conventional approaches are not adequate. To cope with this issue, this paper proposes a new approach based on the idea that a stiffer cell will receive more drag force due to a smaller deformation when it passes through a narrow throat. We suppose both a microchannel with throat and a high speed vision system for observing the cell behavior. When a cell is passing through a channel whose diameter is smaller than the cell, it receives a drag force depending upon both the size and the stiffness. If we can suppose that each cell has a constant size, which is not the case in actual situation, the passing time will eventually depend upon the stiffness. In case that the size varies from cell to cell, it of course depends upon the size as well as the stiffness. This means

that we can evaluate the cell stiffness by measuring both the passing time and the size of cell before entering the channel. There are two challenges; one is whether we can confirm an appropriate correlation among the cell stiffness, cell diameter and the passing time, and the other is whether we can measure both the diameter and the passing time in real time or not. This paper is organized as follows. After briefly reviewing related works in Section II, we explain the basic working principle of the key idea in Section III. Then, we describe our experimental system in Section IV, where a couple of behaviors of cell in the microchannel are shown. Finally, we give some discussions before concluding remarks.

II. RELATED WORKS

There are two approaches for measuring stiffness of the object; one is direct method [10]–[15] where the stiffness is directly evaluated by measuring both contact force and deformation of the object. The feature of direct method is that highly accurate experimental results can be obtained, for example, by establishing mechanical model of a cell [16], [17]. The other is indirect method [18]–[22] where the stiffness is evaluated indirectly, such as by observing the behavior of object without measuring both the deformation and the force imparted to the object. Our approach is categorized into the indirect method. Compared with any direct method, an indirect method enables us to evaluate the stiffness with a shorter time in general.

As for a high speed vision, Ishikawa and Ishii are pioneers for designing the software as well as the hardware [23]–[26]. In order to reduce the computation burden, they propose a window based approach where they focus on a small searching area including the target object. This idea is based on the fact that the object movement should be small enough to ensure the object being always within the window when we increase the frame rate. For example, under the infinite frame rate, the object will never be away from the window whose size is even one pixel bigger than the object. They applied it for various fields, such as high speed robots, virtual instruments, games, and sensing and control of micro living thing under microscopic capturing. We have also implemented a high speed vision to various robots, such as, the 100G Capturing Robot [27], and the Pizza Manipulation [28], by using the algorithm proposed by Ishikawa and Ishii. As for a cell sorter, an extremely high speed cell sorting system is being developed [29]. An inappropriate cell judged by an optical checker is electrically charged in the next channel and then the particular cell is selected quickly by the help of electromagnetic force, as shown in Fig. 2.

III. THE BASIC WORKING PRINCIPLE

Let us explain the working principle by using a 2D model as shown in Fig. 1, where D_0 , B , l , h , τ , and U are the initial diameter of cell, the width of channel, the length of the channel, the gap between the cell and the wall of channel, a shearing stress, and the mean velocity of cell in channel, respectively. Through a deformation of cell, a cell can pass

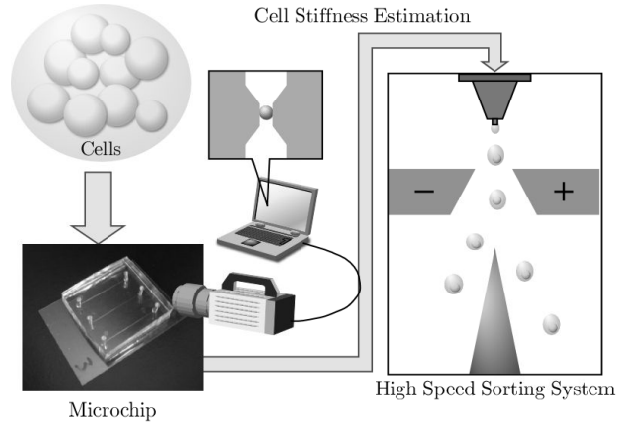


Fig. 2. An overview of cell sorting system implemented our channel

through a channel even when the size is smaller than that of the cell. In case that the size of channel is larger than the cell, the passing time is even shorter than the case where it is smaller than the cell. Thus, we can easily discriminate cells whose sizes are smaller than that of channel. From now on, we suppose that the size of cell is a bit larger than the channel, which means that each cell is compulsorily making deformation when passing the channel, as shown in Fig. 1 or it is completely in stuck at the entrance in case that the cell is big enough or stiff enough. Here, we handle the case where a cell is passing through the channel successfully. Suppose that $D_0 \approx 5$ [μm], $U \approx 10$ [mm/s], and kinematic viscosity coefficient of water $\nu \approx 0.9$ [mm^2/s], respectively. Under this condition, the Reynolds Number $Re \approx 0.056$, under which a laminar flow is guaranteed between a cell and the wall of channel. By considering this condition, we can easily obtain the linear flow pattern $u(y)$ [30], as shown in Fig. 1.

$$u(y) = \frac{Uy}{h} \quad (1)$$

where y is the coordinate whose origin is the wall of the channel. The shear stress τ is given by,

$$\tau(y) = \mu \frac{du}{dy} \quad (2)$$

where μ is the coefficient of viscous friction. Putting (1) into (2) yields,

$$\tau(y) = \frac{\mu U}{h} \quad (3)$$

The drag force F_d produced by τ is given by

$$F_d = \frac{\mu\pi ULB}{h} \quad (4)$$

Since the drag force expressed by (4) balances with the force produced by a pressure drop between the upper flow and the down flow, we eventually have the following relationship,

$$\frac{\Delta P \pi B^2}{4} = \frac{\mu\pi ULB}{h} \quad (5)$$

From (5), we can obtain,

$$U = \frac{\Delta P h B}{4\mu L} \quad (6)$$

where μ , L , and ΔP can be regarded as constant, respectively. Furthermore, since U can be replaced by $U = \frac{l}{T}$, (6) can be rewritten into

$$T = \frac{C}{h} \quad (7)$$

where $C = \frac{4\mu L}{\Delta P B}$. Equation (7) means that the passing time T is inversely proportional to h . Now, the important factor is h indicating the gap between cell and the wall of channel. The gap is physically a fluid micro film, just like an oil film appearing between a ball and supporting house of bearing system. While the film cannot be described by a simple closed form, the normal force to the wall strongly makes influence on the film. By considering this, we can rewrite h by using elastic modulus and initial diameter of cells.

$$h = f(K, D_0) \quad (8)$$

Therefore, by combining both (7) and (8), we can finally obtain,

$$K = g(T, D_0) \quad (9)$$

A normal force $F_n \sim K(D_0 - B)$. This means that a larger stiffness K leads to a larger normal force and a larger D_0 produces a larger force as well. This understanding quite matches with our intuition. For obtaining a relationship between K and T , suppose that $h \sim \frac{1}{F_n} \sim \frac{1}{KD_0}$. As a result, (7) results in,

$$T \sim CKD_0 \quad (10)$$

Equation (10) can be rewritten by

$$K \sim \frac{T}{CD_0} \quad (11)$$

We believe that this relationship is really informative, even though this is just a simple model under the assumption that the thickness of fluid film is inversely proportional to the force due to deformation. The simple model tells us that cell stiffness is simply proportional to T , and inversely proportional to D_0 .

IV. EXPERIMENTS

A. Experimental System

Fig. 3 shows an overview of the experimental system which is composed of a microchip including microchannel, a syringe for supplying a fluid with cells, a microscope for visually enlarging the test bed, and a high speed camera for measuring both D_0 and T . The microchip with the channel width of 6 $[\mu\text{m}]$ is shown in Fig. 4 includes two holes where one is for supplying fluid and the other is for discharging fluid. In order to keep ΔP constant, the pushing velocity of syringe should also be kept constant. To do this, we utilize the syringe control system, as shown in Fig. 5. As for the microscope, we utilize the phase-contrast microscope IX71 (Olympus Co. Ltd.) with visual amplification of 100 times. With the utilization of such a microscope, the velocity of cell in the microscope is also amplified with 100 times, which means that a cell moving with the speed of 10 $[\text{mm}/\text{sec}]$ is observed with the velocity of 1 $[\text{m}/\text{sec}]$ in the microscope.

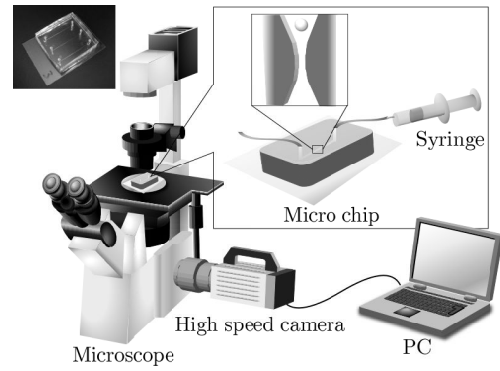


Fig. 3. An overview of the experiment system

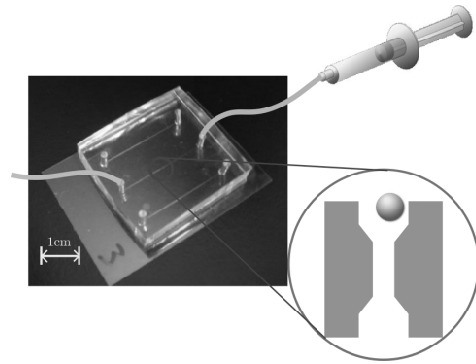


Fig. 4. An overview of microchip

This is the reason why we are planning to implement a high speed vision system with real time processing. However, in this work, we implement a high speed camera (Nac Co. Ltd.) with the speed of 10,000 [frames/sec] instead of such a high speed vision, so that we can observe what are really happening in the channel. Yeast cells with their sizes of 3 through 10 $[\mu\text{m}]$ are utilized for this experiment. As for the high speed camera, we set with the frame rate of 8000 [frames/sec]. In experiment, T is defined by the time passing into the throat whose width is reduced by 10 % compared with the normal channel.

B. Fabrication of Microchannel

To produce the PDMS (Polydimethylsiloxane) microchannel, the photolithography technique is applied. First of all, we spin coat a thick negative photoresist SU-8 3035 (Nippon Kayaku Co.) on a silicon substrate (3 [cm] x 3 [cm]) with a speed of 4000 [rpm] for 20 [s]. Then the substrate is exposed with 400 $[\text{mJ}/\text{cm}^2]$ (i-line 365 [nm]). The height of the SU-8 microchannel fabricated with the condition above was 25 $[\mu\text{m}]$. After that the SU-8 microchannel is transcribed by PDMS to produce PDMS microchannel. The PDMS microchannel is plasma bonded with a cover glass. Finally the PDMS microchannel with a bonded cover glass is put on the hotplate (150 $[\text{C}]$, 30 [min]) for a permanent bonding. This process is shown in Fig. 6

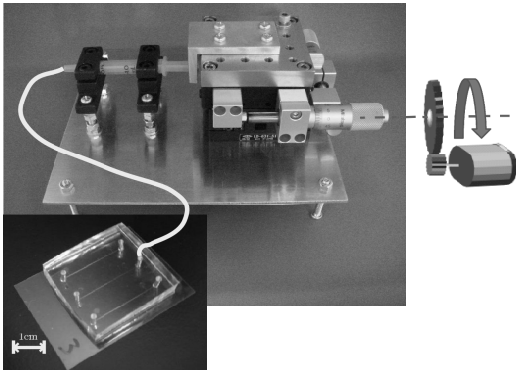


Fig. 5. Syringe control system

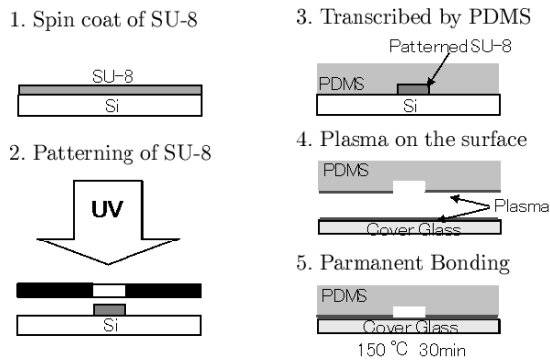


Fig. 6. Fabrication of PDMS microchannel

C. Experimental Results

A series of continuous pictures of yeast cells obtained by the high speed camera are shown in Fig. 7, where (a), (b), and (c) are results for $D_0 = 6.1 \text{ } [\mu\text{m}]$, $D_0 = 8.1 \text{ } [\mu\text{m}]$ and $D_0 = 8.0 \text{ } [\mu\text{m}]$ with respect to time, respectively. Every picture in (a), (b), and (c) is so arranged that each horizontal line of pictures may exhibit the position of cell at the same time. From these figures, we can see that it takes more time for a cell with $D_0 = 8.1 \text{ } [\mu\text{m}]$ to pass the channel than that with $D_0 = 6.1 \text{ } [\mu\text{m}]$, as expected. Fig. 8 shows the relationship between D_0 and T . From Fig. 8, we can see that T increases comparatively sharply with respect to D_0 in the range of $D_0 > 6 \text{ } [\mu\text{m}]$, while T is almost constant in $D_0 < 6 \text{ } [\mu\text{m}]$. We would note that there are a couple points with different T for the nearly same D_0 . Those cells are possible candidates where they have different stiffness. When we compare the pictures (b) and (c) in Fig. 7, even though the cell of (c) is a little smaller than the one of (b), it took more passing time. Furthermore, when we look at the pictures 3–5 of (c), we can note that the cell of (c) almost stays at the throat though it is very short time. From these results, we can assume that the cell of (c) is harder to deform at the throat than the one of (b), and the time difference between (b) and (c) may come from the difference of stiffness, while we can not declare it since we do not know the stiffness of each cell under the current experiments.

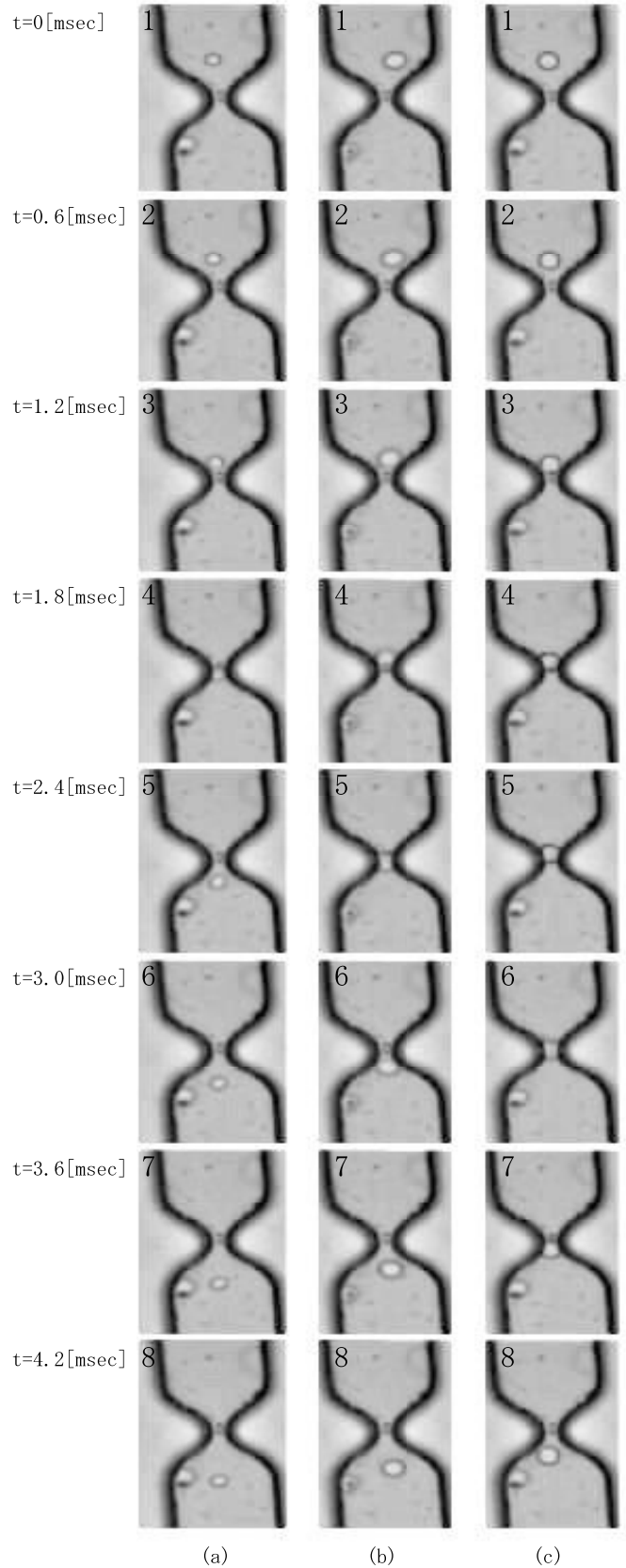


Fig. 7. Cell behavior in the microchannel: (a) $D_0 = 6.1 \text{ } [\mu\text{m}]$, (b) $D_0 = 8.1 \text{ } [\mu\text{m}]$ and (c) $D_0 = 8.0 \text{ } [\mu\text{m}]$, $B = 6.0 \text{ } [\mu\text{m}]$

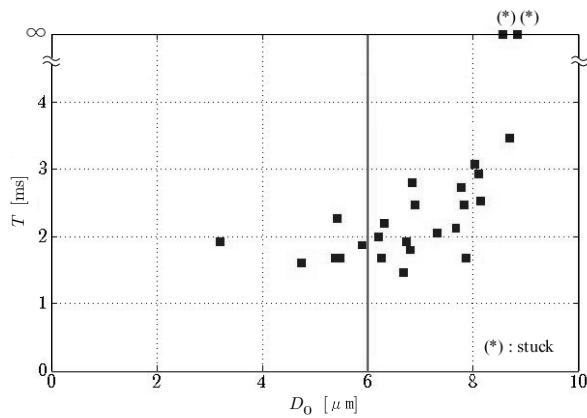


Fig. 8. The relationship between the initial diameter and the passing time of cells

V. DISCUSSIONS

There are two further issues toward the implementation for connecting to a cell sorter. One is on-line classification by using a high speed vision instead of a high speed camera. The other is the confirmation of the relationship between the stiffness and two other factors, T and D_0 , by using cells whose stiffness is known. As for the first issue, the searching line should be fixed by just two pixel lines as shown in Fig. 9, where the horizontal and the vertical lines are for measuring the diameter and for the passing time, respectively. This two-line algorithm will greatly contribute to the processing time cut. Instead of measuring the initial diameter D_0 , the length of cell in passing the test channel may be utilized for evaluating the size of cell. In order to handle more cells/sec, we can set the channels with throat in parallel, as shown in Fig. 10. By adopting this parallel channels system, we can pursue the measurement even if some of the channels are stuffed by cells and this factor makes the processing time per one cell more shorten. As for the second issue, we first plan to make experiments by using artificial beads whose stiffness is known, so that we can confirm whether it is possible to evaluate K from both T and D_0 and obtain the independent correlations between K and T . As the next step, we prepare an AFM for obtaining a referenced stiffness for comparison purpose. Another interesting observation may be expected for the cell behavior, especially in recovery phase, because a cell recovers into the original shape by its own elastic force after passing the throat. While a cell is compulsorily deformed by the shape of throat, we may be able to observe the inherent impedance in the cell dynamics during the recovery phase as we can see it in human skin behavior during air puff impartment [19]. This behavior could suggest us with another index for evaluating the activity of cell in more direct manner. Fig. 7 shows just two examples where (b) and (c) have the nearly same D_0 but different T , respectively. From Fig. 11, we can see how the recovery phase looks like. Ohba et. al. measured the recovery time after red blood cells pass through

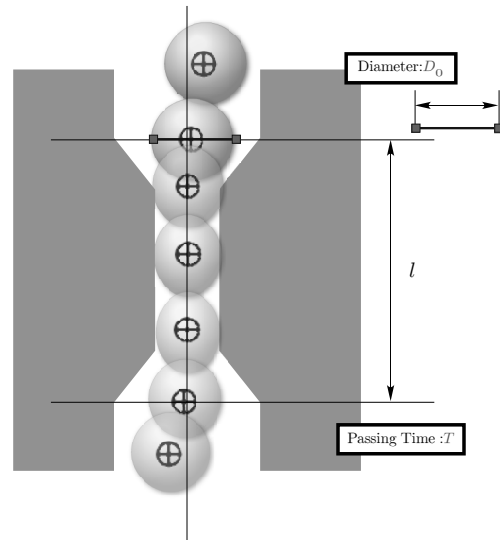


Fig. 9. A concept of the on-line measurement

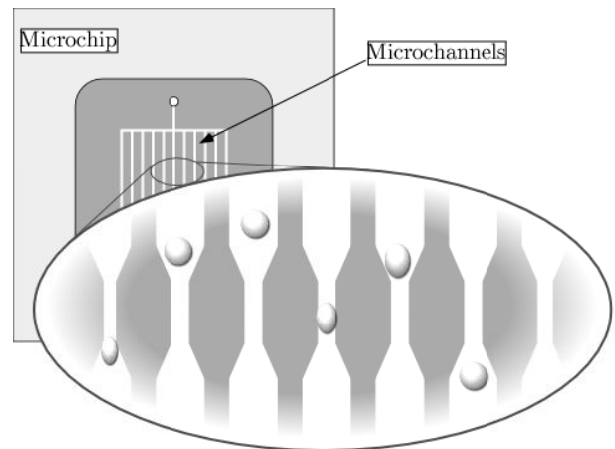


Fig. 10. Parallel channels system

a microchannel by using a high speed camera. Through experiments, they showed the relationship between the time constant and the mean velocity in a channel of erythrocytes, for both healthy person and diabetic person, respectively. As a result, they found that red blood cells become harder in diabetic person than those in healthy person, though the sampling number is not enough for guaranteeing the result [31]. We believe that either the passing time or the recovery time constant should be a good index for evaluating the stiffness of cell appropriately.

VI. CONCLUDING REMARKS

We have proposed a new approach for evaluating cell stiffness K , which is possibly applicable to the cell sorter. What we have done are summarized as follows.

(1) We showed that cell stiffness can be a function of both

the diameter of cell D_0 and the passing time T , and under the assumption that the thickness of fluid film between cell and the wall is inversely proportional to the force due to the cell deformation, K is proportional to T .

(2) We constructed an experimental system and confirmed the basic idea experimentally through off-line computation by utilizing a high speed camera.

(3) We suggested that the dynamics of recovery phase after throat could be also an index for evaluating the activity of cell. For future works, we are planning to make experiments by using artificial beads whose stiffness is known, so that we can confirm whether it is possible to evaluate K from both T and D_0 . Furthermore, we would replace the high speed camera by high speed vision with appropriate algorithm. This work is partially supported by g-COE "in-Silico Medicine (Osaka University)".

REFERENCES

- [1] K. R. Chien, "Regenerative medicine and human models of human disease," *Nature*, Vol. 453, pp. 302–305, 2008.
- [2] H. J. Rippon and A. E. Bishop, "Embryonic stem cells," *Cell Proliferation*, Vol. 37, pp. 33–34, 2004.
- [3] K. Takahashi, K. Tanabe, M. Ohnuki, M. Narita, T. Ichisaka, K. Tomoda and S. Yamanaka, "Induction of Pluripotent Stem Cells from Adult Human Fibroblasts by Defined Factors," *Cell*, Vol. 131, No. 5, pp. 861–872, 2007.
- [4] G. Binnig, C. F. Quate, and Ch. Gerber, "Atomic Force Microscope," *Physical Review Letters*, Vol. 56, No. 9, pp. 930–933, 1986.
- [5] J. L. Alonso and W. H. Goldmann, "Feeling the forces: atomic force microscopy in cell biology," *Life Sciences*, Vol. 72, pp. 2553–2560, 2003.
- [6] S. E. Cross, Y. S. Jin, J. Rao, and J. K. Gimzewski, "Nanomechanical analysis of cells from cancer patients," *Nature Nanotechnology*, Vol. 2, pp. 780–783, 2007.
- [7] E. P. Wojcikiewicz, X. Zhang, and V. T. Moy, "Force and Compliance Measurements on Living Cells Using Atomic Force Microscopy (AFM)," *Biological Procedures Online*, Vol. 6, pp. 1–9, 2004.
- [8] T. Oie, Y. Maruyama, T. Fukuda, C. Nagai, S. Omata, K. Kanada, H. Yaku, and Y. Nakata, "Local elasticity imaging of vascular tissues using a tactile mapping system," *Journal of Artificial Organs*, Vol. 12, pp. 40–46, 2009.
- [9] K. Nagayama, S. Yanagihara, and T. Matsumoto, "A novel micro tensile tester with feed-back control for viscoelastic analysis of single isolated smooth muscle cells," *Medical Engineering & Physics*, Vol. 29, pp. 620–628, 2006.
- [10] N. Tanaka, M. Higashimori, and M. Kaneko, "Active Sensing for Viscoelastic Tissue with Coupling Effect," *30th Annual International Conference of the IEEE Engineering in Medicine and Biology Society (EMBC2008)*, pp. 106–111, 2008.
- [11] S. Katakura, H. Tsukamoto, E. Sugimoto, K. Kobayashi, Y. Kurita, Y. Iida, R. Kempf, J. Okude, M. Kaneko, and H. K. Mishima, "Ocular Stiffness Measurement using Goldmann Applanation Tonometer," *XVII International Congress of Eye Research (ICER2006)*, MO24, 2006.
- [12] T. Kawahara, S. Tanaka, and M. Kaneko, "Non-Contact Stiffness Imager," *The International Journal of Robotics Research*, Vol. 25, No. 5/6, pp. 537–549, 2006.
- [13] T. Kawahara, K. Tokuda, N. Tanaka, and M. Kaneko, "Noncontact Impedance Sensing," *The Int. J. of Artificial Life and Robotics*, Vol. 10, pp. 35–40, 2006.
- [14] Y. Kurita, R. Kempf, Y. Iida, J. Okude, M. Kaneko, H. K. Mishima, H. Tsukamoto, E. Sugimoto, S. Katakura, K. Kobayashi, and Y. Kiuchi, "Contact Based Stiffness Sensing of Human Eye," *IEEE Transactions on Biomedical Engineering*, Vol. 55, No. 2, pp. 739–745, 2008.
- [15] E. Sugimoto, H. Tsukamoto, J. Takenaka, S. Mukai, H. K. Mishima, K. Tokuda, T. Kawahara, and M. Kaneko, "New technique for measurement of ocular stiffness by dynamic analysis in human," *Association for Research in Vision and Ophthalmology 2005*, p. 4851, 2005.
- [16] Y. Sun and B. J. Nelson, "Biological cell injection using autonomous microrobotics system," *The Int. J. Robotics Research*, Vol. 21, pp. 861–868, 2002.
- [17] Y. Tan, D. Sun, W. Huang, and S. H. Cheng, "Mechanical modeling of biological cells in microinjection," *IEEE Transactions on Nanobiotechnology*, Vol. 7, No. 4, pp. 257–266, 2008.
- [18] M. Kaneko, C. Toya, and M. Okajima, "Active Strobe Imager for Visualizing Dynamic Behavior of Tumors," *Proc. of the 2007 IEEE International Conf. on Robotics and Automation*, pp. 3009–3014, 2007.
- [19] N. Tanaka and M. Kaneko, "Skin Surface Shock Wave," *2006 IEEE Engineering in Medicine and Biology Annual Conference (EMBC2006)*, pp. 4123–4126, 2006.
- [20] N. Ueno, M. Kaneko, and M. Svinin, "Dynamic Active Antenna Considering with Multi Oscillation Models," *Journal of Advanced Robotics*, Vol. 15, No. 1, pp. 61–67, 1997.
- [21] N. Ueno, M. Svinin, and M. Kaneko, "Dynamic Contact Sensing by Flexible Beam," *IEEE/ASME Transactions on Mechatronics*, Vol. 3, No. 4, pp. 254–264, 1998.
- [22] M. Kaneko, N. Kanayama, and T. Tsuji, "Active Antenna for Contact Sensing," *IEEE Transactions on Robotics and Automation*, Vol. 14, No. 2, pp. 278–291, 1998.
- [23] T. Komuro, I. Ishii, M. Ishikawa, and A. Yoshida, "A digital vision chip specialized for high-speed target tracking," *IEEE Trans. Electron. Devices*, Vol. 50, pp. 191–199, 2003.
- [24] I. Ishii and M. Ishikawa, "High speed target tracking algorithm for 1 ms visual feedback system," *J. Robotics Soc. Japan*, Vol. 17, pp. 39–45, 1999.
- [25] I. Ishii, K. Kato, S. Kurozumi, H. Nagai, A. Numata, and K. Tajima, "Development of a Mega-pixel and millisecond Vision System using Intelligent Pixel Selection," *TEXCRA2004*, pp. 9–10, 2004.
- [26] K. Tajima, A. Numata, and I. Ishii, "Development of a high-resolution, high-speed vision system using CMOS image sensor technology enhanced by intelligent pixel selection technique," *Optics Ea 2004, Proc. SPIE*, Vol. 5603, pp. 215–224, 2004.
- [27] M. Higashimori, M. Kaneko, A. Namiki, and M. Ishikawa, "Design of the 100G Capturing Robot Based on Dynamic Preshaping," *The International Journal of Robotics Research*, Vol. 24, No. 9, pp. 743–753, 2005.
- [28] M. Higashimori, K. Utsumi, and M. Kaneko, "Dexterous Hyper Plate Inspired by Pizza Manipulation," *Proc. of the IEEE Int. Conf. on Robotics and Automation (ICRA08)*, pp. 399–406, 2008.
- [29] S. F. Lbrahim and G. V. D. Engh, "High-speed cell sorting: fundamentals and recent advances," *Current Opinion in Biotechnology*, Vol. 14, pp. 5–12, 2003.
- [30] F. M. White, "Viscous Fluid Flow," pp. 426–428, 1974.
- [31] Y. Imamura, T. Tajikawa, K. Ohba, and T. Takubo, "Measurement of the time constant of shape recovery of human erythrocyte using a micro-channel technique," *Mechanical Engineering Congress 2009*, Vol. 6, No. 09-1, pp. 197–198, 2009.

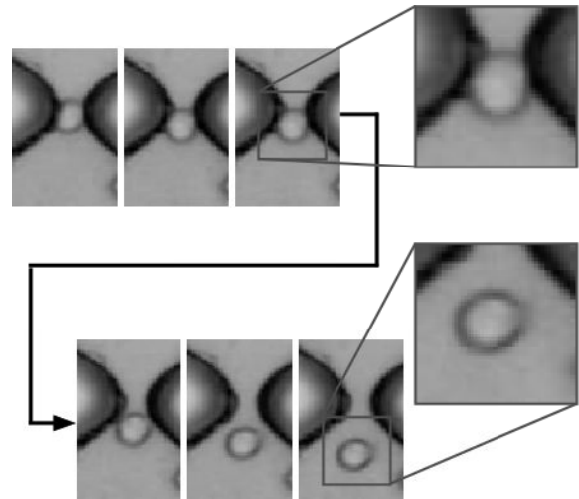


Fig. 11. Cell recovery phase